RESEARCH ARTICLE

Evolving Teeth Within a Stable Masticatory Apparatus in Orkney Mice

Sabrina Renaud[1] · Ronan Ledevin[1,2] · Louise Souquet[1,3] · Helder Gomes Rodrigues[4,5,6] · Samuel Ginot[3,6] ·
Sylvie Agret[6] · Julien Claude[6] · Anthony Herrel[5] · Lionel Hautier[6]

Abstract
Mice from the Orkney archipelago exhibit an important diversity regarding molar shape. While on some islands mice display a usual dental pattern, teeth from other islands display additional cusplets and unusual phenotypes that may constitute case studies for evaluating the potential functional relevance of dental changes. We developed a multifaceted approach combining 2D and 3D geometric morphometrics, dental topography, dental wear, biomechanics, estimations of masticatory muscles force, and in vivo bite force on wild-derived lab descendants exemplifying the two extreme dental morphologies. The two strains differed in the geometry of the upper and lower tooth rows, and in the topography of the upper row only. Surprisingly, the most unusual tooth morphology appeared as the least complex because tooth simplification overwhelmed the signal provided by the occurrence of additional cusplets. No difference in bite force nor muscle force was evidenced, showing that the important change in dental morphology was accommodated without major changes in the rest of the masticatory apparatus. The evolution of unusual dental phenotypes was possibly fueled by drift and inbreeding in small and isolated populations on remote islands of the archipelago. No functional counter-selection impeded this diversification, since the unusual dental phenotypes did not disrupt occlusion and mastication.

Keywords Adaptation · Biomechanics · Biting · Functional morphology · Molar · Mandible · *Mus musculus domesticus* · Rodent

✉ Sabrina Renaud
   sabrina.renaud@univ-lyon1.fr

1   Laboratoire de Biométrie et Biologie Evolutive, UMR 5558, Université Lyon 1, CNRS, 69100 Villeurbanne Cedex, France

2   Present Address: UMR5199 PACEA, Université de Bordeaux, Allée Geoffroy Saint Hilaire (Bat. B8), 33615 Pessac, France

3   Present Address: Institut de Génomique Fonctionnelle de Lyon, UMR 5242, CNRS, Ecole Normale Supérieure de Lyon, Université Claude Bernard Lyon 1, 46 Allée d'Italie, 69364 Lyon Cedex 07, France

4   Centre de Recherche sur la Paléobiodiversité et les Paléoenvironnements (CR2P), UMR CNRS 7207, CP38, Muséum national d'Histoire naturelle, Univ Paris 6, 8 rue Buffon, 75005 Paris, France

5   Mécanismes adaptatifs et évolution (MECADEV), UMR 7179, CNRS, Funevol team, Muséum National d'Histoire Naturelle, 55 rue Buffon, Bat. Anatomie Comparée, CP 55, 75005 Paris Cedex 5, France

6   Institut des Sciences de l'Evolution, Université de Montpellier, UMR5554 CNRS, IRD, EPHE, Place Eugène Bataillon, CC65, 34095 Montpellier Cedex, France

Introduction

Phenotypic variation is a key feature in evolution because it is the raw material upon which selection acts. Being the product of stochastic genetic changes, phenotypic variation can be channeled by development and/or genetic covariation into preferred directions constituting 'lines of least resistance to evolution' (Schluter 1996) that may favor response to selection if both directions are aligned. Phenotypic variation can also arise due to phenotypic plasticity, in which case it is directly related to environmental cues (West-Eberard 1989). It can then favor evolution by rapidly producing adaptive phenotypes (Scoville and Pfrender 2010). In all these contexts, an adaptive interpretation of phenotypic evolution is often tempting, especially if it is supported by cases of convergent evolution (Harmon et al. 2005). However, lines of least resistance to evolution can also channel the repeated but independent evolution of some phenotypes even without similar selective pressures. Independent evidence of the functional relevance of the phenotypic traits involved is thus crucial to support adaptive interpretations.

The mammalian dentition is thought to have evolved in response to selective pressures related to feeding strategies, with constraints related to phylogenetic history and development (Jacobs et al. 1990; Jernvall 2000). In rodents, the acquisition and development of ever-growing incisors favored evolution towards an increased incisor efficiency and induced a major rearrangement of the masticatory muscles (Wood 1965). In particular, the evolution of the masticatory apparatus in murines has been channeled towards the acquisition of the propalinal chewing movements (Lazzari et al. 2008). As a consequence, selection was not focused on single morphological traits (e.g. number of cusps on the molar teeth) but involved a series of integrated phenotypic changes involving osteological, myological, and dental features. Strong functional constraints affecting mastication limit the number of possible evolutionary pathways of the tooth rows, as only a restricted set of murine dental morphotypes permit antero-posterior movements for gnawing and chewing. Within the framework of these functional constraints, some liberty exists for dental innovations that do not disrupt the biomechanics of the whole masticatory apparatus. Such 'non-disruptive pathways', where a morphological change can be functional for one aspect (e.g. a dental change improving the efficiency of occlusion) but neutral for others aspects of mastication (e.g. the dental change does not impede the propalinal movement) are of major concern for the understanding of diversification in a constrained functional context.

With an increasing knowledge on tooth development, it has appeared that some unusual phenotypes, such as accessory cusps, may be easily produced by small differences in the inhibitory field surrounding the main forming cusps, thus explaining how populations can be polymorphic for such traits (Charles and Viriot 2015; Salazar-Ciudad and Jernvall 2002). Variance due to the occurrence or not of such an additional cusplet at the anterior part of the first upper molar tooth has been shown to be favored by development, resulting in the repeated evolution thereof (Renaud et al. 2011). The anterior position of the additional cusplet, in front of the occlusion with the lower molar, may have allowed it to evolve without disrupting the functioning of the masticatory apparatus (Renaud and Auffray 2013).

The evolution of this anterior cusplet seems to have occurred most frequently on islands (Ledevin et al. 2016; Renaud et al. 2011). It is unclear, however, if these cases of parallel evolution correspond to adaptive evolution or not, since insular contexts can also favor random evolution due to founder effects and drift in small, isolated populations (Berry 1996). Surfing on developmental lines of least resistance may then cause parallel evolution even without involving adaptation. On the other hand, ecological conditions on islands depart from those prevailing in source populations on the continent, thus promoting adaptive evolution.

The question is therefore whether the phenotypic changes involved may confer, or not, an adaptive advantage.

Recent findings evidenced such dental variation within Orkney house mice (*Mus musculus domesticus*) (Ledevin et al. 2016). On some islands, phenotypes with the additional cusplet prevail (Fig. 1), while these are almost absent on other islands. Following a field trip in 2012, wild-trapped mice from such contrasted populations were used to found two strains where active selection was applied to fix each phenotype (presence/absence of the cusplet). The descendants from the strains were bred under similar laboratory conditions, discarding sources of variations such as plastic variation in response to different environments. Comparing a set of descendants of the two strains, with and without the additional cusplet, we developed a multifaceted approach including 2D and 3D morphometrics and biomechanics to address the following questions. (1) Can the differences in dental phenotype be of functional significance, and can they constitute an adaptive advantage in some environmental conditions? We addressed these questions by using analyses of tooth microwear and macrowear, and by assessing tooth sharpness, complexity and relief based on topographic parameters derived of 3D imagery of the molar rows. (2) How are differences in tooth morphology accommodated by the osteological and muscular components of the masticatory apparatus? These questions were addressed by combining quantitative approaches of four components: assessment of tooth geometry in 2D and 3D, quantification of mandible shape and biomechanics using 2D morphometrics, estimation of masticatory muscle forces based on dissections, and in vivo measures of bite force.

Material

Wild mice were trapped during a field trip to the Orkney Islands (North of Scotland) in 2012. Two islands were sampled: Papa Westray and South Ronaldsay. South Ronaldsay is the most southern island of the archipelago. Relatively large (4980 ha), it has a moderate human population density (~ 18.3 habitant/km^2) and a good potential for exchange with the main island of the archipelago since causeways built during World War II provide road access from Mainland to South Ronaldsay. Papa Westray, in contrast, is one of the most northern islands of the Orkneys. It is small (918 ha) and less populated (~ 9.8 habitant/km^2) than South Ronaldsay. It can only be reached by small ferry boats, and is therefore relatively isolated.

Fourteen mice were captured on Papa Westray and 27 on South Ronaldsay. A part of the mice (i.e. two mice from Papa Westray and seven from South Ronaldsay) was euthanized during the field expedition. The rest was brought to the rodent breeding facilities at the University
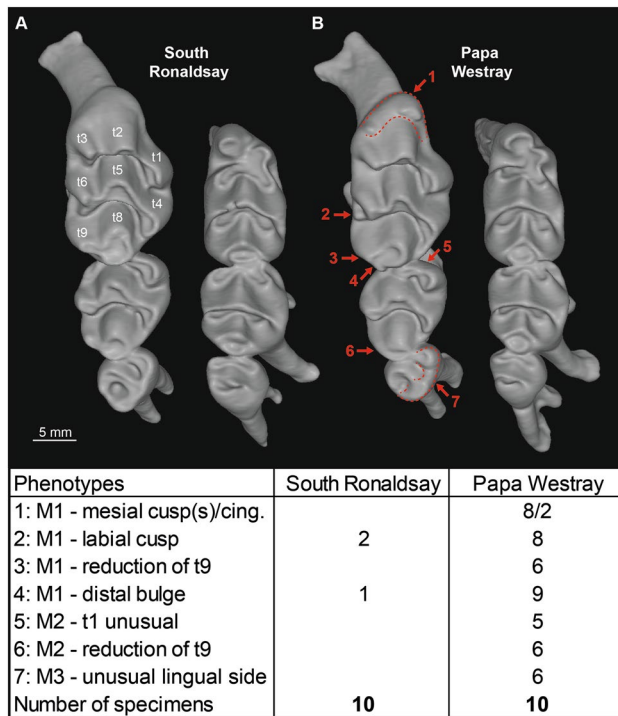
Fig. 1 Upper and lower molars of different mice populations from Orkney Islands, and associated frequencies of the different unusual phenotypes observed. **a** Upper and lower dental rows of a specimen from South Ronaldsay (SR1031), and associated nomenclature. **b** Upper and lower dental rows of a specimen from Papa Westray (PW0511). Images correspond to X-Ray microtomographic 3D renderings of the molar rows

Phenotypes	South Ronaldsay	Papa Westray
1: M1 - mesial cusp(s)/cing.		8/2
2: M1 - labial cusp	2	8
3: M1 - reduction of t9		6
4: M1 - distal bulge	1	9
5: M2 - t1 unusual		5
6: M2 - reduction of t9		6
7: M3 - unusual lingual side		6
Number of specimens	**10**	**10**

of Montpellier, France (CECEMA). These individuals were used as founders of two inbred strains: PW, derived from four Papa Westray founders, and SR, derived from eight South Ronaldsay founders. Papa Westray and South Ronaldsay populations display a different morphology of the first upper molar, mice from South Ronaldsay displaying a rather typical tooth morphology while PW molars show an anterior elongation up to the occurrence of an additional cusplet (Fig. 1). The two strains were actively selected for the fixation of this character in the PW strain, and for its absence in the SR strain.

For morphometric analyses, ten specimens were selected from each strain. They corresponded to the second to the sixth generation of laboratory crosses (Table 1). About half of the mice were young adults (between 67 and 73 days) and the other half were older animals up to about 6 months.

The morphology of these animals bred in the laboratory was compared to the one of the mice trapped in 2012, which include animals sacrificed in the field and the founders of the colonies.

The mice were sacrificed according to the directive 2010/63/UE of the European Parliament on the protection of animals used for scientific purposes.

Methods

Qualitative Characterization of the Tooth Phenotype and Wear Assessment

For the set of wild-derived laboratory mice (10 PW, 10 SR), skulls were scanned at a cubic voxel resolution of 12 µm using a Phoenix Nanotom S microtomograph (µCT) on the AniRA-ImmOs platform of the SFR Biosciences, Ecole Normale Supérieure, Lyon (France).

The right upper molar row (UMR) and the right lower molar row (LMR) were delimited on each slice using a threshold method in Avizo (v. 9.1—Visualization Science Group, FEI Company). In most cases, an automatic threshold was sufficient to isolate the molar rows from the surrounding bone and generate a surface including the roots; in a few cases corresponding to old mice, connections with the bone had to be manually delimited.

Based on these 3D models, phenotypes of upper and lower molars were described and compared. The dental nomenclature follows (Miller 1912).

Next, dental macrowear and microwear analyses were performed to detect evidence of attrition and abrasion on the extra anterior (mesial) cusps on first upper molars (UM1) and to test the putative masticatory role of this additional cusp. To do so, casts of first upper molars were investigated in six specimens with the best developed anterior cusplet (PW0351, PW0352, PW0484, PW0493, PW0511, and PW0512). Their mesial part was digitized using transmitted light stereomicroscopy with a protocol adapted to the small dentition of rodents using a ×100 magnification (Gomes Rodrigues et al. 2009). Based on these data, traces of wear were qualitatively assessed.

2D Tooth Shape

The first upper molars (UM1) were photographed while being oriented so that the occlusal surface would match at best the horizontal plane. Right molars were considered, except when missing or broken; a mirror image of the left one was then measured. Based on these photographs, the shape of the UM1 was described using 64 points sampled at equal curvilinear distance along their 2D outline using the image analysis software Optimas. The starting point

Table 1 Specimens of the strains PW and SR analyzed in this study, with age, geometric and topographic characteristics of the molar rows, bite force, force of the main masticatory muscles, and mechanical advantage (MA) of the temporal/incisor (Temp/Inc) and masseter/molar (Mass/Mol) complex

Individual	Strain	Age	Fn	Sex	Upper molars					Lower molars					Bite force	Muscle force				MA	
					Shape		Topography			Shape		Topography				Mass	Temp	ZI	PTE	Temp/Inc	Mass/Mol
					PC1	PC2	DNE	OPCR	RFI	PC1	PC2	DNE	OPCR	RFI							
PW351	PW	190 (130)	4	M	−0.018	−0.020	594	223	0.409	−0.021	−0.026	567	205	0.393	10.7	6.11	3.73	1.08	2.83	0.191	0.594
PW352	PW	190 (130)	4	F	−0.004	−0.014	565	217	0.401	−0.007	−0.019	562	196	0.407	8.5	6.62	2.19	1.98	3.49	0.184	0.542
PW484	PW	95 (61)	5	F	0.004	−0.016	669	203	0.433	0.010	−0.020	606	175	0.397	5.1	5.63	2.83	1.23	2.88	0.223	0.524
PW493	PW	90 (29)	5	M	0.004	−0.008	657	213	0.424	0.008	−0.015	694	193	0.414	6.2	5.03	1.86	1.09	2.60	0.239	0.508
PW511	PW	73	5	M	0.020	−0.009	698	203	0.440	0.028	0.000	694	185	0.425		6.97	3.01	1.14	3.62	0.181	0.570
PW512	PW	73	5	F	0.018	−0.011	730	197	0.427	0.033	−0.005	642	181	0.400		6.27	2.63	1.08	2.65	0.186	0.516
PW844	PW	69	5	F	0.020	−0.005	730	229	0.400	0.029	−0.011	662	182	0.402	7.6	5.51	2.46	1.51	1.65	0.221	0.520
PW845	PW	69	5	M	0.018	−0.007	702	192	0.426	0.025	−0.021	717	200	0.413	9.6	7.08	2.56	1.51	3.14	0.215	0.568
PW855	PW	67	6	M	0.004	−0.004	615	198	0.404	0.015	−0.009	631	198	0.411	7.7	6.17	3.32	1.42	3.53	0.202	0.511
PW1157	PW	70	5	M	0.014	−0.003	679	211	0.433	0.022	−0.006	666	198	0.421	8.2	6.04	2.87	1.78	2.99	0.201	0.469
SR292	SR	207	2	F	−0.015	0.005	670	228	0.420	−0.034	0.009	617	187	0.412	9.4	7.31	3.59	1.52	3.09		
SR302	SR	206	3	F	−0.019	−0.003	698	230	0.402	−0.037	0.005	582	181	0.408	7.4	7.84	2.71	1.28	2.46	0.227	0.528
SR321	SR	184	3	M	−0.023	−0.002	644	257	0.420	−0.067	−0.006	595	206	0.377	8.1	6.69	2.45	1.69	2.84		
SR324	SR	183	3	F	−0.017	−0.003	688	229	0.424	−0.031	−0.000	590	196	0.404	4.2	5.81	2.38	1.93	2.57	0.224	0.519
SR413	SR	122 (94)	3	F	−0.017	0.001	811	248	0.437	−0.023	0.004	685	195	0.394	8.1	5.44	2.63	1.47	2.39		
SR502	SR	73 (18)	3	F	0.003	0.009	854	238	0.445	0.008	0.021	670	184	0.398	3.2	5.21	2.46	1.50	3.00	0.239	0.540
SR1031	SR	71	4	F	0.006	0.027	843	231	0.446	0.017	0.029	765	232	0.407	7.1	5.82	2.31	1.50	3.06	0.253	0.533
SR1033	SR	71	4	F	0.007	0.023	788	224	0.433	0.010	0.021	697	187	0.404	6.2	5.86	2.31	1.29	2.42	0.230	0.493
SR1083	SR	68	3	M	−0.001	0.023	821	222	0.439	0.010	0.024	714	193	0.422	9.9	6.99	3.27	1.83	3.70	0.245	0.526
SR1084	SR	68	3	M	−0.003	0.020	742	229	0.436	0.003	0.027	675	194	0.411	10.2	8.32	2.91	1.76	3.11	0.209	0.515

Age: age at sacrifice (in brackets: age at bite force measurement, when different), Fn: generations in the lab, Shape (PC1 and PC2 scores) and topographic parameters (DNE, OPCR and RFI) are provided for the upper molar row and the lower molar row, Muscle force: estimated force of the main masticatory muscles (*mass* masseter, *temp* temporal, *ZI* zygomatic, *PTE* pterygoid), *MA* mechanical advantage

was manually positioned at the anteriormost part of the tooth.

From the 64 points, 64 radii (i.e. distance of each point to the center of gravity of the outline) were computed. Expressed as a function of the curvilinear distance along the outline, this set of radii constituted a function that was analyzed using a Fourier analysis (Rohlf and Archie 1984). The empirical function (radius as a function of the curvilinear distance) is decomposed into a sum of trigonometric functions of decreasing wavelength (the harmonics). Each is weighed by two Fourier coefficients (FCs) that constitute the shape variables to be compared among individuals. The zero harmonic (A0) is proportional to the average radius and hence to the size of the outline. It was used to standardize all other FCs so that they represent shape only. This Fourier analysis was performed using the 'sfourier' function using the Momocs package 1.1.6 (Bonhomme et al. 2014) in R (R-Core-Team 2017).

The higher the rank of the harmonics, the more details they represent on the outline (Crampton 1995; Rohlf and Archie 1984) and the less information they bring. This can be used to filter measurement error and reduce the number of variables by discarding high-order harmonics (Renaud et al. 1996). Considering the cumulative power (i.e. information brought by each successive harmonic), it appeared that the molar tooth could be adequately described by the first seven harmonics, i.e. by 14 variables (FCs), representing more than 99% of the total information (function cumulative_power in Momocs).

The 64 points along the outline are enclosed into a bounding box (i.e. the smallest rectangle that enclosed the object delineated by the points). The length and width of this bounding box provided an estimate of these dimensions for each tooth (function coo_lw in Momocs).

The analysis was performed on the tooth of the wild and laboratory mice (61 UM1). The shape variables (FCs of the first seven harmonics) were summarized using a principal component analysis (PCA) performed on the variance–covariance matrix of the FCs. PCA allows for a visualization of the principal axes of shape variation, and for a reduction of dimensionality (Sheets et al. 2006). Differences between groups (wild PW, wild SR, laboratory PW, laboratory SR) were tested using analyses of variance (ANOVA) and post-hoc Tukey tests for univariate size estimates (tooth length and width). Shape differences were tested using a multivariate analysis of variance (MANOVA) and pairwise Hotelling's T^2 tests on the set of PC axes explaining more than 5% of the total variance.

3D Characterization of the Upper and Lower Molar Rows

Mouse molars are composed of transverse enamel ridges (Fig. 1), the cusps of which align to form longitudinal rows that guide the propalinal (antero-posterior) movement during chewing. The molar row has a complex geometry which prevents to reliably locate landmarks and delineate curves along the ridges (Skinner and Gunz 2010). Thus, we developed a method of shape description that relies on the description of the molar row surface (Renaud and Ledevin 2017). A template of the upper molar row was designed on a randomly chosen specimen (SR292) to describe the entire erupted crown. This template was defined by 2917 equally-spaced sliding semi-landmarks anchored by 11 fixed landmarks. These fixed landmarks were defined on all specimens and were only used as priors to guide the registration process. The template was deformed in order to match the original surface of each tooth row (Ledevin et al. 2016). An iterative procedure was used to slide points along tangent planes according to the minimum bending energy criterion until convergence (Gunz et al. 2005). Next, the resulting sliding semi-landmarks were adjusted for scaling, translation, and rotation according to a Procrustes superimposition. These procedures were performed using the packages 'Morpho' (Schlager 2017) and 'mesheR' (Schlager 2016). Procrustes coordinates, i.e. coordinates of the sliding semi-landmarks after Procrustes superimposition, constituted the shape variables describing the shape of the tooth row.

The same procedure was applied to the lower molar row (LMR), with a template of 2927 sliding semi-landmarks and 11 fixed landmarks.

As for the 2D outline analysis, the shape variables (here the Procrustes coordinates of the 2917 semi-landmarks for the upper molar row, and 2927 for the lower molar row) were described and summarized using a principal component analysis (PCA). A pairwise Hotelling's T^2 test was performed using as variables the set of PC axes explaining more than 10% of the total variance. This threshold was chosen to limit the number of variables due to the reduced number of specimens and the large number of original variables included in the 3D analysis.

Topographic Analysis of the Upper and Lower Molar Rows

The topographic parameters were computed from the templates of the upper and lower molar rows used for the geometric morphometric assessment of their shape. The templates were used to discard the root portions of the original surface that would otherwise cause errors during computation of the complexity parameters.

To circumvent the uncertainty in the estimation of the topographic parameters related to inconsistencies in the manual orientation of the molar rows, a four-step semi-automatic procedure was developed (Renaud and Ledevin 2017). First, a surface of reference was randomly chosen (here, SR292) and manually aligned in space using Avizo (v 9.1) so that the occlusal surface would be aligned with the X and Y planes, lying face-up, and oriented orthogonal to the Z-axis. Next, the auto3dgm R package (Boyer et al. 2015) was used to automatically align all remaining dental surfaces and the reference surface using a Procrustes superimposition. Third, the difference in position between the reference surface before and after the Procrustes superimposition was calculated. The same transformation was applied to the remaining dental row surfaces with the goal to orient them exactly as the reference surface, with the occlusal surface facing up, while retaining the Procrustes superimposition. Finally, these surfaces were simplified to 10,000 polygonal faces (Pampush et al. 2016) using the R package Rvcg (Schlager 2017).

Three parameters were used to characterize the topographic properties of the molar rows. Dirichlet normal energy (DNE) assesses tooth sharpness by measuring the curvature and undulation of the surface (Bunn et al. 2011). Orientation patch count (OPC) estimates the number of separately oriented facets on a tooth surface (Evans et al. 2007) and is considered a proxy for dental complexity (Santana et al. 2011). It is measured by dividing a tooth surface into contiguous patches that share an orientation and then summing the number of such patches. Because counts may vary depending on the orientation of the occlusal surface, we used a variant of the method [orientation patch count rotated (OPCR)] (Evans and Jernvall 2009) measuring complexity by starting from the initial orientation, rotating the surface by 5.625° a total of eight times around the Z-axis, and averaging the resulting OPC estimates to provide the OPCR value. The third parameter, Relief Index (RFI), corresponds to the log ratio between the surface area of a tooth's crown (Area3D) and the area of the tooth planometric footprint (Area2D) (Boyer 2008).

The estimations of DNE, OPCR, and RFI were performed using the R package molaR (Pampush et al. 2016).

Mandible Shape

Mandibles were photographed after being put flat on their lingual side. Left mandibles were considered, except when damaged; the mirror image of the right one was then measured. The shape of the mandible was described using 64 points sampled at equal curvilinear distances along their 2D outline, the starting point being positioned at the dorsal junction between the incisor and the mandibular bone. Using the Momocs package (Bonhomme et al. 2014), the outlines were then centered, scaled, and aligned along their long axis. They were then analyzed using an elliptic Fourier transform (Kuhl and Giardina 1982) (efourier in Momocs). This method decomposes the variations of x- and y-coordinates as functions of the curvilinear abscissa along the outline. Each function is decomposed into a sum of trigonometric functions of decreasing wavelength (the harmonics) weighed by two Fourier coefficients (FCs), so that together, each harmonic is weighed by four coefficients (two for x, two for y). It is particularly efficient for describing complex shapes such as the mandible. Mandible shape could be adequately described by the first seven harmonics, representing more than 95% of the total information.

This analysis was performed on the mandible of the wild and laboratory mice (59 mandibles). The set of FCs was summarized using a principal component analysis (PCA) performed on the variance–covariance matrix of the FCs.

The mandibular bone can change plastically throughout the life of the animal in response to muscular and external loads (Renaud et al. 2010). For the analysis of mandible shape, we therefore considered separately the animals sacrificed during the 2012 field trip, and those that were brought back. A limit is the low sample size for the wild groups (PW: 2; SR: 7). Differences between groups (wild PW and SR sacrificed just after capture; wild PW and SR brought to the lab; laboratory descendants of PW and SR) were tested using an analysis of variance (ANOVA) and post-hoc Tukey tests on a univariate size estimate (mandible area). Shape differences were tested using a multivariate analysis of variance (MANOVA) and pairwise Hotelling's T^2 tests on the set of PC axes explaining more than 5% of the total variance.

Biomechanical Analysis of the Mandible

The mechanical advantage is a measure of the efficiency of mandible geometry to transmit force from the muscles to the bite point. It can be estimated as the ratio of the in-lever (distance from the condyle to the point of muscle attachment) and the out-lever (distance from the condyle to the bite point) (Hiiemae 1971). Out-levers were estimated as the distance from the condylar articulation to the incisor tip, and to the first molar main cusp (hypoconid). Regarding in-levers, the effect of the superficial masseter was approximated by considering the distance from the condyle to the posterior tip of the angular process. The distance from the condyle to the tip of the coronoid described the action of the temporalis (Anderson et al. 2014; Renaud et al. 2015). The temporalis is mostly used together with incisors for gnawing; whereas the masseter and molars are involved in the action of mastication. Two mechanical advantages were therefore considered: temporalis/incisor, masseter/molar. As for mandible shape, six groups were considered: wild PW and SR

sacrificed just after capture; wild PW and SR brought to the lab; laboratory descendants of PW and SR. Differences were tested using an analysis of variance (ANOVA) and post-hoc Tukey tests.

Bite Force

Bite force was measured using a Kistler piezo-electric force transducer (Anthony Herrel et al. 1999). The same user (SG) performed all the measurements to avoid inter-user error. Each mouse bit three times in a row and only its highest bite force was selected to be used in the following analyses. For a few mice, the age when bite force was measured was not the age of sacrifice (Table 1).

Dissection and Muscle Forces

After bite force measurements specimens were sacrificed, heads were fixed during 48 h in 4% formol, and thereafter conserved in 70% alcohol. The masseter, temporal, zygomatico-mandibularis, and pterygoid muscles were dissected and weighed. Each muscle was then submerged in a nitric acid solution (HNO_3 30%) for 24 h to separate muscular fibers and then covered with a 50% aqueous glycerol solution. For each muscle, ten fibers were chosen haphazardly, drawn and measured using the ImageJ software (Abramoff et al. 2004). The mean fiber length was estimated for each muscle. The cross sectional area of the muscle was approximated by the muscle volume ratio, obtained by dividing the weight by the muscular density, taken here as 1.06 g/cm^2 (Anthony Herrel et al. 2008; Murphy and Beardsley 1974), subsequently divided by the mean fiber length. An estimate of the muscle force can then be obtained by multiplying this section by the muscle stress, taken here as 25 N/cm^2 (Anthony Herrel et al. 2008).

Statistical Tests of the Differences Between the PW and SR Strains

Differences between the two strains were tested for topographic parameters of the molar rows, bite force, muscle forces, and mechanical advantages using t-tests that perform well even with very small sample sizes (de Winter 2013). Nevertheless, because of the limited sample size, tests may lack statistical power. This issue was assessed using the R package pwr (Champely 2018).

ANOVA (type I sum of squares), pairwise Tukey tests, and t-tests were performed using R (R-Core-Team 2017). PCAs were performed using the R package ade4 (Dray and Dufour 2007). Shape differences were investigated using MANOVA (type I sum of squares) and Hotelling's T^2 tests

on the set of PC axes > 10% of variance. These tests were performed using PAST (Hammer et al. 2001).

For all variables investigated here, variation in individual age may interfere with differences between strains. Linear models including age, strain, and their interaction were therefore also investigated. The percentage of variance explained (pve) by each explanatory variable (age and strain) and the associated probability were assessed using the R package ffmanova (Langsrud and Mevik 2012). This method is based on type II sum of squares, which has the advantage of being invariant to ordering of the model terms; the ffmanova also handles colinear responses. It may inflate the pve but allows an estimation of the relative importance of the explanatory variables. The interaction was never significant, possibly because of small sample size, and was finally discarded from the models.

Results

Dental Phenotypes and Wear of the Additional Cusplet

Observations of dental rows in mice from the Orkney Islands revealed that unusual phenotypes occurred much more frequently on upper molars of specimens from Papa Westray than from South Ronaldsay, while lower molars of both groups appeared less variable (Fig. 1). All investigated PW mice have either a cingulum or more frequently one or several small cusps located at the anterior part of their UM1 (phenotype 1 on Fig. 1). This phenotype is regularly combined with a labial cusp on UM1 (phenotype 2), which is generally connected to the crest starting from the t6. The t9 is often reduced (phenotype 3), and accompanies a more or less marked bulge generally located on its distal margin. On UM2, unusual phenotypes of t1 occasionally occur (phenotype 5), especially on the medial part, while reduction of t9 is more frequent (phenotype 6). On UM3, the lingual cusps display unusual phenotypes (e.g. connection of t1–t4 missing to faintly marked), and distal cusps can be reduced to missing (e.g. t8; phenotype 7). Conversely, only a few of these phenotypes occur on SR mice, and in far lower extent (e.g. rare labial cups, and distal bulge on UM1).

Evidence of dental macrowear and microwear was observed on the tips of most of the extra mesial cusps in all of the PW specimens investigated (Fig. 2). Macrowear corresponded to enamel-free areas and can be observed on the larger extra cusps (Fig. 2b). Microwear features are generally represented by scratches on extra cusps (Fig. 2c).
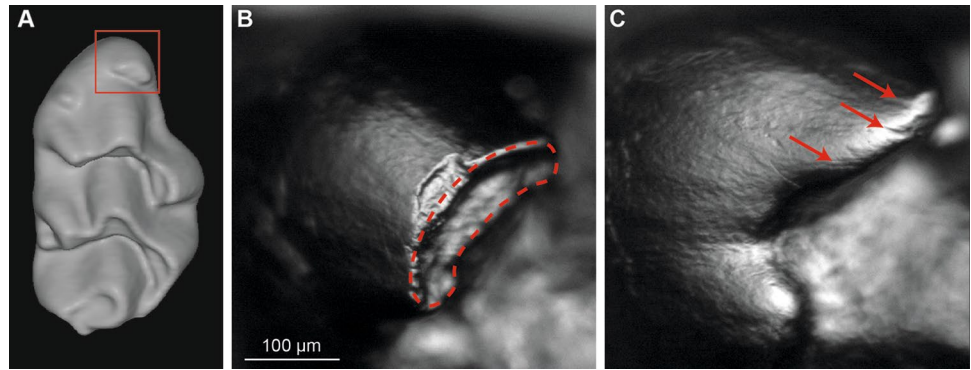
Size and Shape of the First Upper Molar: 2D Characterization and Comparison with Wild Populations

The size of the UM1 was first characterized by the length and width of its 2D outline (Fig. 3a, b). The UM1 of the wild populations from Papa Westray and South Ronaldsay differed in their length but not in their width (Table 2), corresponding to elongated UM1 in PW. The lab PW UM1 were slightly longer than their wild counterparts. The lab SR UM1 were both longer and wider than their wild counterpart. This ended up in PW and SR lab UM1 being different in their length but not their width, as for the wild populations.

Regarding UM1 shape (Fig. 3c), the variation along PC1 (45.5% of total variance) roughly opposed PW teeth, characterized by a slender and elongated outline, to SR teeth that are broad and massive. PC2 (23.6%) corresponded to more or less prominent labial cusps. Lab SR descendants tended to be more extreme than the wild SR along this axis.

Overall, while some overlap existed between teeth of wild-trapped PW and SR mice, lab teeth from PW and SR were fully segregated along a PC1–PC2 diagonal. Four axes explained more than 5% of variance (PC1 = 45.5%, PC2 = 23.6%, PC3 = 9.8%, PC4 = 5.5%). MANOVA and Hotelling's T^2 test were performed on this set of axes. Teeth from PW and SR appeared to be significantly different between the wild specimens, and this significant difference was maintained, or even increased, in the lab descendants (Table 2).

Shape of the Upper Molar Row: 3D Characterization

The upper molar rows were differentiated according to two directions of shape changes (Fig. 4a). Mostly along the first PC axis (35.9% of the total variance), molar rows were ordinated according to the age of the mice, for both PW and SR strains. Accordingly, the first axis mainly corresponded to a pattern of abrasion (Fig. 4b). The PW and SR strains were opposed along the second PC axis (20.9%). Compared to

SR, PW molar rows were characterized by an elongated first molar, and a reduced second molar.

Accordingly, the two strains differed in shape (Table 3). Because the pattern of variation with age is slightly oblique along PC1 and PC2, strains differed along both axes (t-tests: PC1, P = .0085; PC2: P = .0005). Using a model combining age and strain, both appeared significant, with age explaining roughly 40% of the variance (Table 4) and strain slightly more.

A similar pattern was found for the lower molar row, with a significant difference between the two strains (Table 3) (Fig. 4c, d). The two strains varied in a parallel way according to the age and hence the degree of wear along the first axis (42.3% of total variance). The second axis (17.2%) opposed the two strains (Fig. 4c). PW displayed reduced second and third molars compared to SR (Fig. 4d). In a combined model, age and strain explained approximately as much variance as for the upper molar row (Table 4).

Topography of the Molar Rows

The differences in geometry of the upper molar rows were associated with differences in topographic parameters (Figs. 5, 6). Although characterized by additional cusplets, PW molar rows were less sharp and less complex (Table 3) than SR molar rows. The difference in relief was not significant between both strains. Changes with age, due to abrasion, also impacted topographic parameters, especially regarding sharpness (DNE) and relief (RFI) (Fig. 5) whereas complexity (OPCR) did not vary with age. Combining both factors, tooth sharpness appeared primarily influenced by strain, whereas relief was primarily influenced by age. Complexity differed between strains and remained constant with respect to abrasion (Table 4).

No significant difference emerged using t-tests when considering topographic parameters of the lower molar (Table 3), probably because differences between strains were minor compared to the effect of abrasion (Table 4).

Fig. 3 Size and shape of the first upper molar of wild PW and SR mice and their descendants in the lab. **a, b** Length and width of the molar. **c** Shape differentiation on the first two axes of a PCA on the Fourier coefficients describing the molar outline. Each dot corresponds to a tooth. Superimposed to the principal plane, reconstructed outlines depicting the shape variation in this plane. Bottom left, graph of the eigenvalues
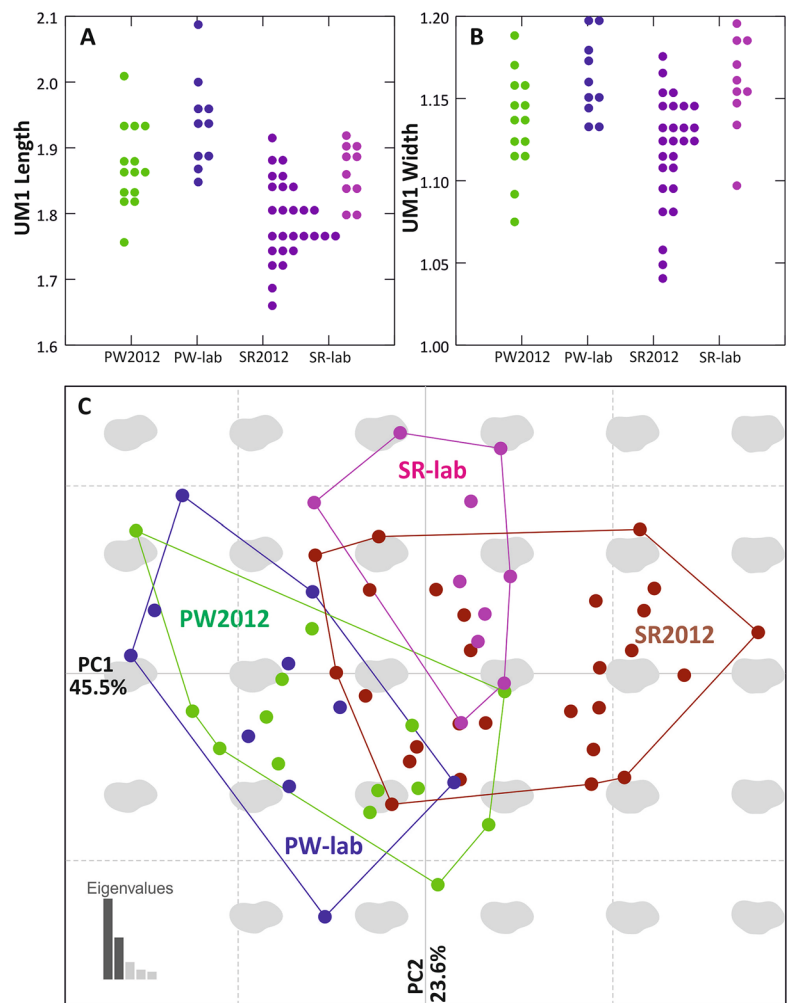
Table 2 First upper molar size and shape differences between the PW and SR laboratory mice, and the corresponding wild populations

ANOVA	df	F			Tukey/Hotelling's T^2					
					PW2012	PW2012	PW2012	SR2012	SR2012	PW_lab
					SR2012	PW_lab	SR_lab	PW_lab	SR_lab	SR_lab
				p (Same)	p (Same)					
Length	3, 57	15.98		**1.17E−07**	*0.0010*	*0.0499*	0.9823	**0.0000001**	*0.0137*	*0.0346*
Width	3, 57	6.794		**.0005389**	0.4041	0.1697	0.2666	*0.0024*	*0.0057*	0.9956
MANOVA	df	F	Wilk's lambda	p (Same)						
PC1, PC2, PC3, PC4	12, 143.2	10.46	0.1891	**1.253E−14**	**<.0001**	0.2282	**<0.0001**	**<0.0001**	**<0.0001**	**<0.0001**

P-values of ANOVAs and associated Tukey's pairwise tests are provided for tooth length and width, and p-values of MANOVA and associated Hotelling's T^2 tests for tooth shape (variables considered were the first four axes of a PCA on the Fourier coefficients, all >5%). In italics P-value < .05. In bold P-value < .001

Regarding the relationships between the two molar rows, sharpness of the lower molar row was correlated to sharpness of its upper counterpart (Pearson's product-moment correlation; UMR DNE vs. LMR DNE: R = 0.7241, P = .0003). Complexity and relief were not related between lower and upper molar rows (Pearson's product-moment

Fig. 4 Geometric differentiation of the upper and lower molar rows between PW and SR lab mice. **a, b** upper molar row. **c, d** Lower molar row. **a, c** Differentiation on the first two axes of a PCA on the shape variables (Procrustes coordinates of the 3D semi-landmarks composing the template). **b, d** Reconstruction of the shape changes along the axes, from positive to negative scores. In red extension, in blue contraction. Groups correspond to the PW and SR strains, split according to the age of the specimens (*Y* young mice of ~70 days, *O* older mice)
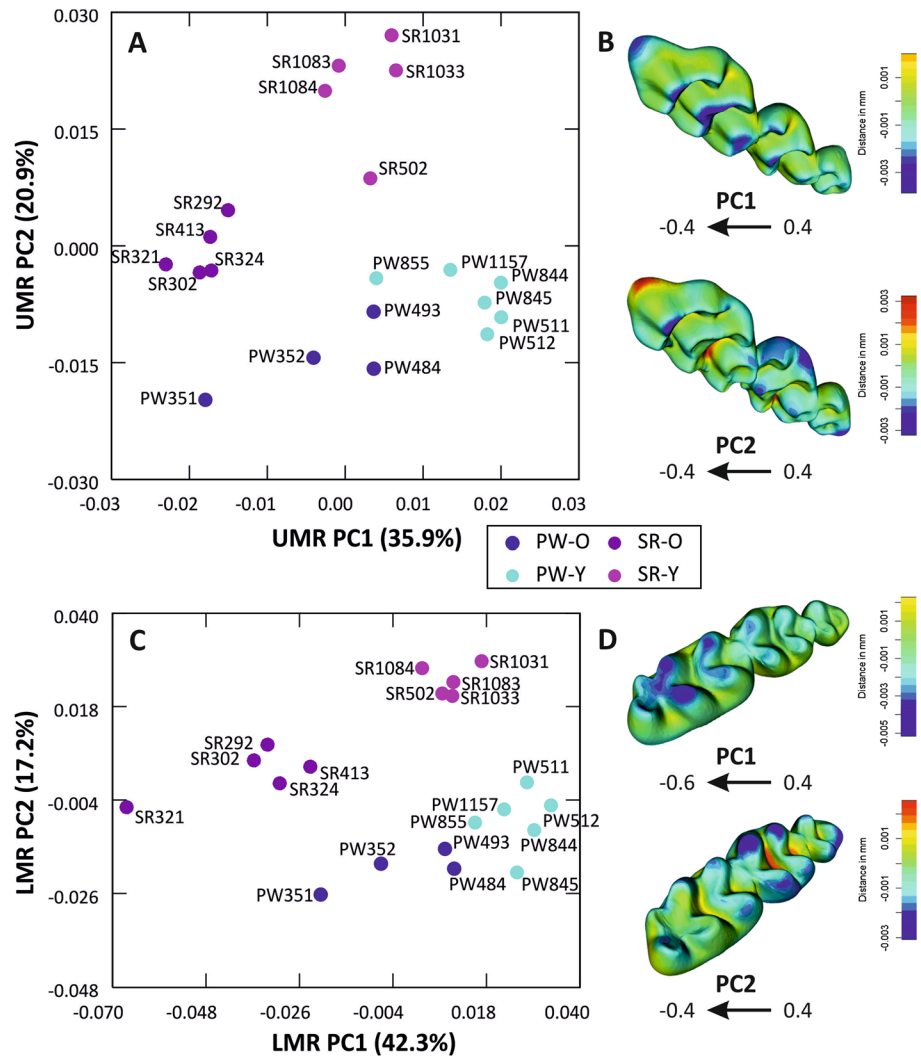
correlation; UMR OPCR vs. LMR OPCR: R = 0.2333, P = .3222; UMR RFI vs. LMR RFI: R = 0.1830, P = .4400).

Mandible Size and Shape: 2D Characterization and Comparison with Wild Populations

Differences in mandible size were documented between groups (Table 5). Wild PW and SR did not differ in mandible size, neither when sacrificed after trapping or when maintained for a while in the lab. Both shared a significant mandible size increase from the wild to the lab probably simply due to aging (Fig. 7a). PW and SR laboratory descendants did not differ in size. Within each strain, descendants did not differ from the size reached by wild-trapped mice kept in the lab.

Differences in mandible shape (Fig. 7b) were tenuous. Wild PW and SR tended to differentiate along the second axis (24.1% of variance). Mandibles of the wild-trapped mice kept in the lab appeared intermediate in shape between the two wild samples. Mandibles of lab descendants of PW and SR strongly overlapped, and seemed shifted along the first axis (43.9%) compared to the wild-trapped individuals brought to the lab.

Three axes each explained more than 5% of variance (PC1 = 43.9%, PC2 = 24.1%, PC3 = 15.2%) and were used in MANOVA and Hotelling's T^2 tests (Table 5). Probably due to small sample size, wild PW and SR failed to be significantly different in mandible shape, despite being close to the significance threshold (P = .0668). Wild-trapped PW and SR brought to the lab exhibited a similar mandible shape (P = .5805). Their lab descendants displayed a slightly different mandible shape (P = .0438).

Biomechanics of the Mandible

Two in-lever/out-lever ratios assessed the efficiency of the mandible shape regarding its two main functions: masseter/molar for chewing and temporal/incisor for

Table 3 Differences between the set of laboratory PW and SR mice

H T^2	df	F	Wilk's lambda	p (Same)
3D UMR				
PC1, PC2	2, 17	58.15	1.28E−01	**2.50E−08**
3D LMR				
PC1, PC2	2, 17	140.5	0.05703	**2.67E−11**

t-Test	df	t		p (Same)
UMR				
DNE	16.527	−3.049		*0.0074*
OPCR	17.863	−4.842		**0.0001**
RFI	17.856	−1.612		0.1245
LMR				
DNE	17.672	−0.588		0.5637
OPCR	15.755	−0.751		0.4637
RFI	17.53	0.861		0.4007
Bite force	15.973	0.583		0.568
Mechanical advantage				
Temporal/Incisor	14.877	−3.433		*0.0037*
Masseter/Molar	12.796	0.790		0.4441
Muscle force				
Masseter	14.781	−0.983		0.3416
Temporal	17.223	0.207		0.8382
Pterygoid	16.249	0.336		0.7410
Zygomatic	16.032	−1.609		0.1272

Differences in molar row geometry were tested using Hotelling's T^2 tests on the sets of PC axes > 10% of variance. Differences in molar row topography (DNE, OPCR, RFI), bite force, mechanical advantages of the mandible, and muscle forces, were tested using t-tests

In italics P-value < .05

In bold P-value < .001

grinding (Fig. 8). When considering all groups including the wild-trapped as well as the lab-reared animals (Fig. 9), the masseter/molar mechanical advantage did not display any difference between groups whereas the temporal/incisor mechanical advantage exhibited some differences (Table 5). In the laboratory descendants, the two mechanical advantages displayed no trend with age (Table 4). The two strains did not differ in their masseter/molar mechanical advantage but SR displayed a slightly higher ratio than PW regarding the temporal/incisor mechanical advantage (Table 3). Note that with a sample size of N = 10 in each group, t-tests are only able to detect differences of 1.3× the pooled standard deviation with a good power (80%).

Considering PW alone, lab descendants displayed a lower ratio than wild PW brought to the lab (P = .0490). The SR groups did not differ in their temporal/incisor mechanical advantage (P = .4016).

Bite Force and Estimated Force of the Masticatory Muscles

Regarding bite force, no clear trend emerged with age, except for one specimen measured while juvenile (18 days) which displayed the lowest bite force (Fig. 10a; Table 4). The two strains did not differ in their bite force (Tables 3, 4).

Four muscles were dissected to extrapolate their force: the masseter, the temporalis, the zygomatico-mandibularis, and the pterygoid muscles (Fig. 8). No variation with age was observed (Fig. 10b–e; Table 4). The two strains displayed similar force values for all muscles (Table 3).

Discussion

Different Tooth Geometry in Orkney Mice

House mice presumably colonized the Orkney Archipelago following the expeditions of the Norwegian Vikings, who

Table 4 Influence of age and strain difference on molar row 3D shape and topography, on mandible mechanical advantages, on masticatory muscle forces, and bite force

	Dependent	Explanatory			
		Age		Strain	
		pve	P-value	pve	P-value
Molar row shape					
UMR	PC1, PC2	**39.6**	**3.6e − 06*****	**43.4**	**8.2e − 08*****
LMR	PC1, PC2	**38.7**	**2.77e − 06*****	**45.8**	**1.25e − 10*****
Topography					
UMR	DNE	**45.4**	**1.09e − 05*****	**53.3**	**4.14e − 06*****
	OPCR	6.0	0.118	**44.9**	**0.000305*****
	RFI	*39.0*	*0.00177***	*24.6*	*0.00912***
LMR	DNE	**70.4**	**4.82e − 06*****	*11.4*	*0.0173**
	OPCR	0.0	0.964	3.0	0.482
	RFI	12.6	0.128	1.1	0.636
Bite force		6.9	0.302	4.9	0?385
Mechanical advantage					
Temporal/ Incisor		6.0	0.227	*43.4*	*0.00432***
Masseter/ Molar		11.6	0.189	3.9	0.434
Muscle force					
Masseter		3.8	0.412	2.9	0.469
Temporal		3.0	0.480	0.8	0.713
Pterygoid		0.6	0.741	0.3	0.816
Zygomatic		0.5	0.756	10.7	0.167

Results of general linear models are provided (*pve* percentage of variance explained). Explanatory variables are age, and strain (PW vs. SR). In bold highly significant P-values (P < .001), in italics P < .05. Interactions were not significant and were discarded from the model

founded settlements in the area (Searle et al. 2009). As a consequence of their common origin, mice from the various islands of the archipelago share a similar haplotypic signature (Ledevin et al. 2016; Searle et al. 2009). Nevertheless, they nowadays display an important tooth shape diversity (Ledevin et al. 2016).

This study focused on mice from two islands from the Orkneys: Papa Westray and South Ronaldsay. Papa Westray mice display one of the most extreme dental phenotypes encountered on the Orkneys (Fig. 1), characterized by additional cusplets, unusual phenotypes and simplification of the dental pattern. South Ronaldsay teeth, in contrast, do not depart markedly from the regular dental pattern of house mice.

Our results first evidenced that laboratory descendants of the mice from Papa Westray (PW) and South Ronaldsay (SR) retained and even increased their dental phenotypic differences, in agreement with the fact that they were progressively inbred, with an active selection for the fixation

of the elongation of the first upper molar for PW and for the absence of this trait for SR.

Three-dimensional imagery allowed to better characterize the geometric differences of the molar tooth rows on a set of laboratory descendants of the PW and SR strains. The presence of an anterior (mesial) additional cusplet on the first upper molar represents the most distinctive phenotypic trait of Papa Westray mice. The evidence of macrowear and microwear on this extra-cusp of PW mice (Fig. 2) suggests that it might participate to the comminution of food particles. Being functional, at least in its most developed form, and heritable, since it could be selected for in the course of artificial breeding, this cusplet could thus be under the screening of selection. This could contribute to explain its recurrent fixation in several fossil (Stoetzel et al. 2013) and extant species of murines (Kan Kouassi et al. 2008), especially within the Murini.

Despite the occurrence of marked phenotypes on the PW upper molars, no obvious qualitative difference existed for the lower molars between the two strains. 3D quantitative analyses nevertheless showed that both molar rows were clearly differentiated between the two strains. The trait most clearly shared by both molar rows was the reduction of the second and third molars in Papa Westray mice. This reduction may be the consequence of a larger first molar, inhibiting the development of the subsequent molars along the cascade of molar development (Kavanagh et al. 2007). This result fits the observation of highly integrated variation between the upper and lower molar rows at the population level (Renaud et al. 2009), despite a higher evolvability of the upper molars (Renaud et al. 2011).

## Relationship Between Geometry and Complexity of the Teeth

The geometric differences were associated with differences in tooth complexity, which were first described in a qualitative way, showing a balance between increased complexity in PW due to additional cusps, and simplifications especially in the posterior region of the teeth. Tooth complexity was also quantified as the number of patches of different orientation on the tooth (Evans and Jernvall 2009; Evans et al. 2007). Differences in quantitative complexity (OPCR) were demonstrated between the upper molar rows of the PW and SR strains. The South Ronaldsay strain appeared to have significantly more complex upper molar rows than the Papa Westray strain. This result points to the fact that the observed unusual phenotypes and simplifications in PW molars overwhelmed the addition of cusplets in the complexity pattern. In agreement with the absence of clear qualitative differences on the lower molar row, no difference in complexity of the lower molar row was demonstrated between the two strains. This provides evidence that the lesser differentiation
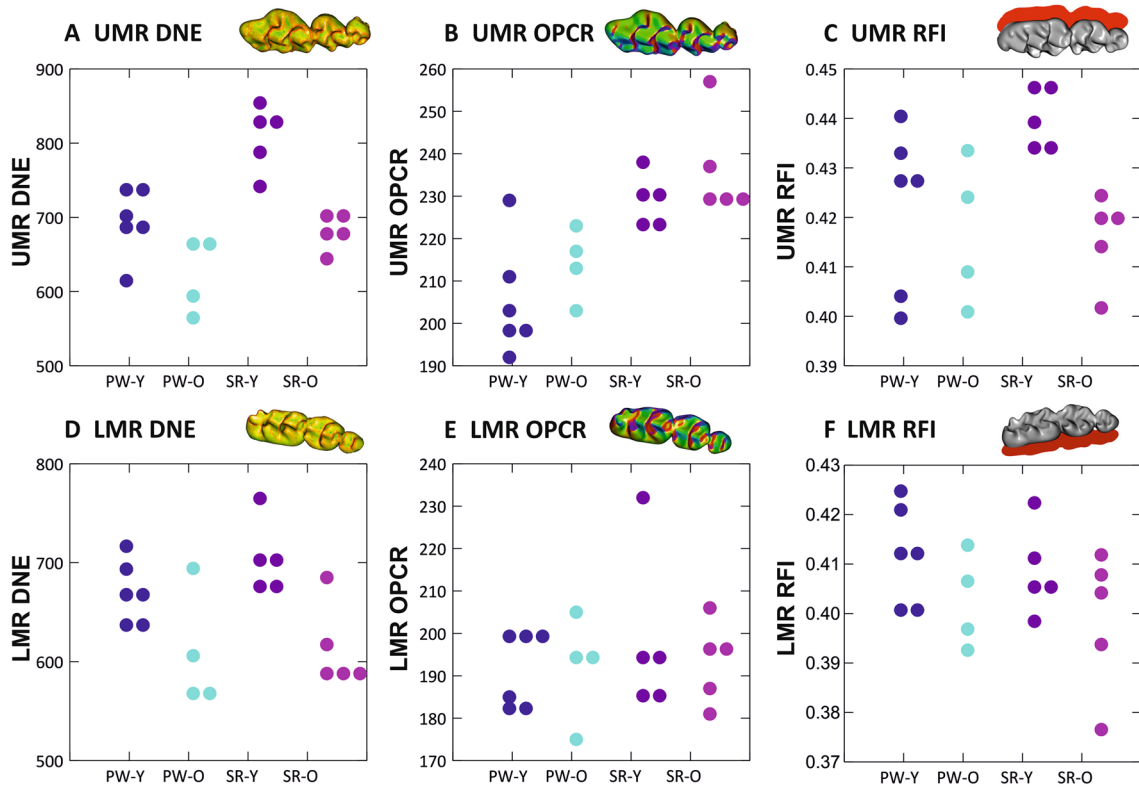
Fig. 5 Topographic signature of the upper and lower molar rows of lab PW and SR. Dental topographic variables were estimated based on a semi-automatic procedure of alignment of the molar rows. **a, d** Tooth curvature (DNE). **b, e** Tooth complexity (OPCR). **c, f** Tooth relief (RFI). **a–c** Upper molar rows. **d–f** Lower molar rows
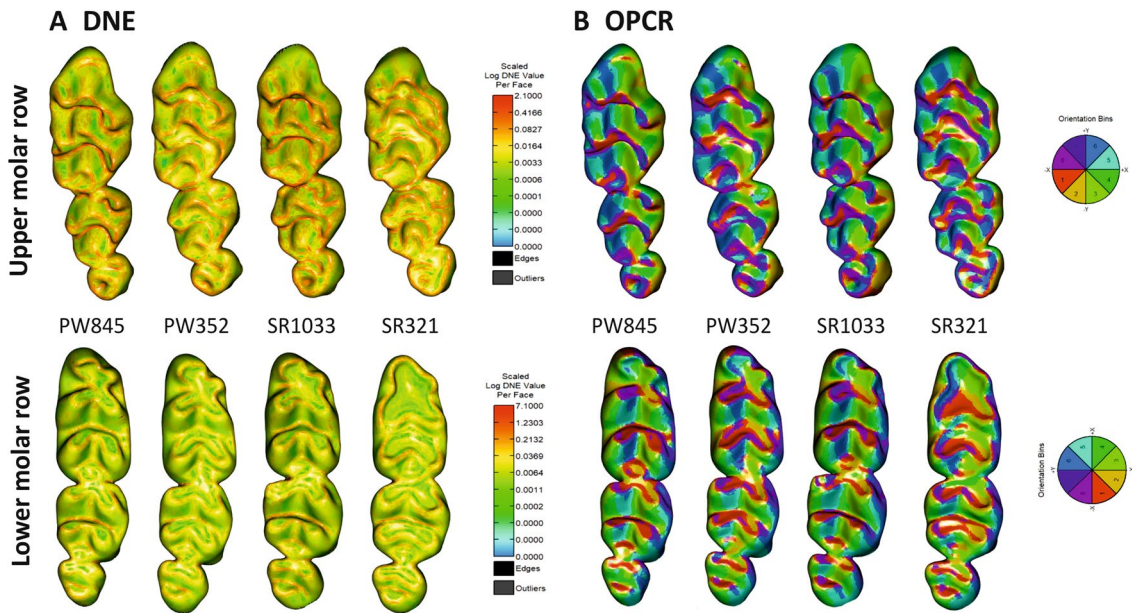
Fig. 6 Visualization of the dental topographic characteristics for four mice exemplifying young and old PW and SR. **a** Tooth curvature (DNE). **b** Tooth complexity (OPCR). Upper panel: upper molar row. Bottom panel: lower molar row. PW845 and SR 1033: mice ~ 70 days of age. PW352 and SR321: mice ~ 190 days of age

Table 5 Differences in mandible size, shape, and mechanical advantages between the PW and SR wild and lab mice

ANOVA	df	F		p (Same)		PW_lab	SR_lab	PW_wlab	PW_wild	SR_wild
Area	5, 53	11.72		1.18E−07	PW_lab					
					SR_lab	1.0000				
					PW_wlab	*0.0095*	*0.0125*			
					PW_wild	0.0885	0.1178	**0.0002**		
					SR_wild	*0.0094*	0.0208	**0.0000**	0.9981	
					SR_wlab	1.0000	0.9998	*0.0023*	0.0558	*0.0017*
MANOVA	df	F	Wilk's L	p (Same)		PW_lab	SR_lab	PW_wlab	PW_wild	SR_wild
PC1, PC2, PC3	15, 141.2	4.562	0.3359	5.02E−07	PW_lab					
					SR_lab	*0.0438*				
					PW_wlab	*0.0028*	*0.0503*			
					PW_wild	0.2890	0.1754	*0.0361*		
					SR_wild	*0.0325*	0.0545	*0.0066*	0.0668	
					SR_wlab	0.0005	*0.0243*	0.5805	*0.0067*	*0.0118*
ANOVA	df	F		p (Same)		PW_lab	PW_lab	PW_lab	PW_lab	PW_lab
MA temp/ inc	5, 51	4.992		.00085	PW_lab					
					SR_lab	0.2375				
					PW_wlab	*0.0346*	0.9968			
					PW_wild	0.9942	0.9552	0.8380		
					SR_wild	*0.0020*	0.4690	0.6267	0.3176	
					SR_wlab	*0.0011*	0.8070	0.9467	0.5585	0.9229
	df	F		p (Same)		PW_lab	PW_lab	PW_lab	PW_lab	PW_lab
MA mass/ mol	5, 51	1.112		.366	PW_lab					
					SR_lab	0.9682				
					PW_wlab	1.0000	0.9754			
					PW_wild	0.6806	0.9337	0.6961		
					SR_wild	0.9300	1.0000	0.9409	0.9668	
					SR_wlab	0.9957	0.7667	0.9880	0.4712	0.6787

Groups are, for PW and SR: mice sacrificed in the field (wild), wild-trapped mice brought back to the lab (wlab), and laboratory descendants (lab). P-values of ANOVAs and associated Tukey's pairwise tests are provided for mandible area, and temporal/incisor and masseter/molar mechanical advantages (MA temp/inc and MA mass/mol). P-values of a MANOVA and associated Hotelling's T^2 tests for mandible shape (variables considered were the first three axes of a PCA on the Fourier coefficients, all > 5%). In italics P < .05, in bold P < .001

in lower molar shape between PW and SR is mirrored by the absence of differences in complexity.

Possible Significance and Limits of the Tooth Topographic Parameters

Dental topography is interpreted as related to dietary specializations across taxa (Bunn et al. 2011; Godfrey et al. 2012; Ungar 2004). Species consuming food items such as tendons, muscles, or insect cuticles, tend to possess molars with high, sharp cusps for puncturing and shearing these materials. Species consuming fruits, or other items requiring to be crushed, tend to have molars with low cusps, open basins, and many facets for gripping and crushing these foods (Evans and Sanson 2003; Winchester et al. 2014). Depending on the diet, different topographic characteristics may present a functional advantage. Overall, herbivorous species consuming food that requires grinding display a higher complexity than carnivores (Evans et al. 2007). Even between related species, high complexity values have been associated to a more fibrous and structural carbohydrate-dominated diet (Boyer et al. 2010; Winchester et al. 2014). Resistance to such an abrasive diet can also be increased by a high relief index (Evans et al. 2007). In contrast, greater sharpness might be of advantage for carnivores, even to the detriment of complexity. Transferring this interpretative

Fig. 7 Size and shape of the mandible of wild-trapped PW and SR mice and their descendants in the lab. **a** Mandible size, estimated by the 2D area of the mandibular bone. **b** Shape differentiation on the first two axes of a PCA on the Fourier coefficients describing the mandible outline. Each dot corresponds to a specimen. Superimposed to the principal plane, reconstructed outlines depicting the shape variation in this plane. Groups correspond, for the PW and SR strains, to wild animals trapped and sacrificed on the field (wild), wild animals brought back to the lab (wild → lab), and lab descendants (lab)
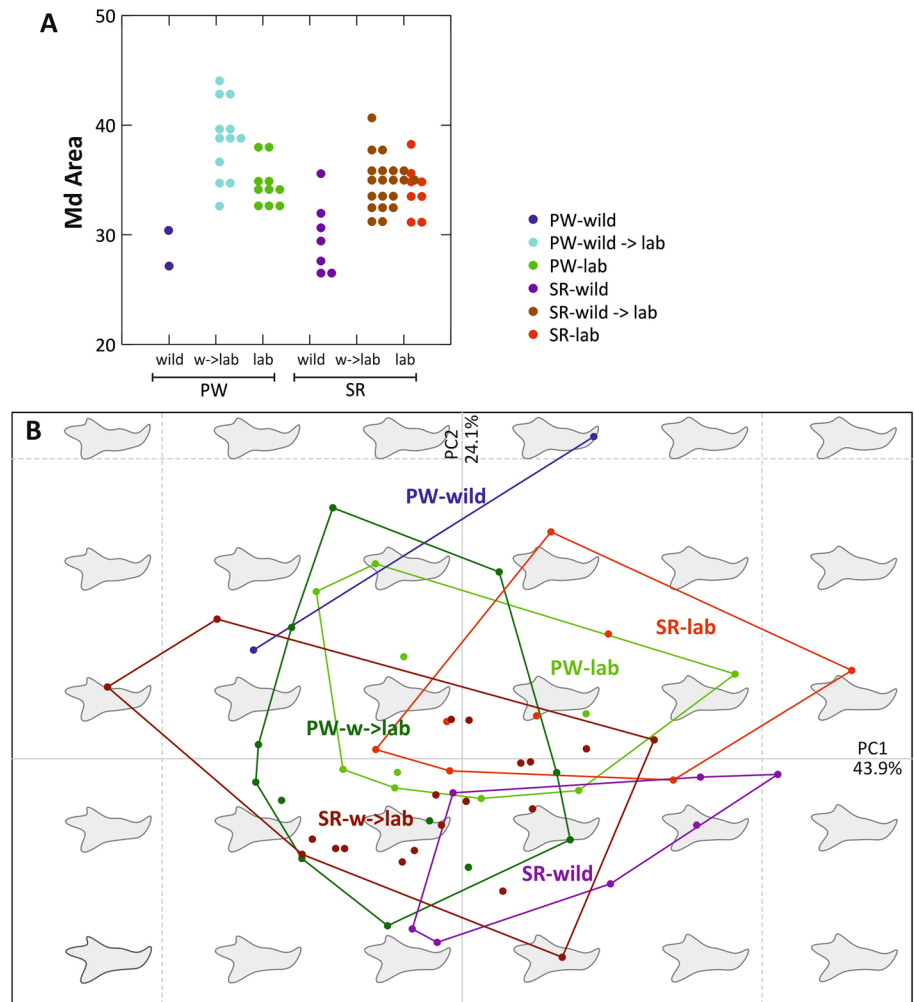
framework to intraspecific differences is, however, limited by the amount of topographic variations due to wear, and hence age, but also individual diet (Renaud and Ledevin 2017).

Our study, however, showed consistent differences in tooth topography between PW and SR mice, especially regarding upper molars. Relief appeared to be mostly driven by age-related variation and hence increased wear, without displaying clear differences between strains. As such, it appears of limited interest for ecological inferences, but it may be useful to estimate the degree of wear in wild populations, for which age is not controlled.

In contrast, PW and SR mice were characterized by consistent differences in complexity and sharpness, PW displaying lower values for both parameters. The signal in sharpness was indeed affected by age-related wear, but this was not sufficient to obliterate the between-strain differences. Dental complexity was not affected by age/wear, as was already observed for laboratory mice (Renaud and Ledevin 2017). This suggests that mouse dentition maintains its complexity with age, despite changes in the

shape of the cusps due to wear. This parameter may thus be particularly relevant for comparing wild populations.

The greater complexity and sharpness of SR teeth compared to PW teeth overall suggests a higher functional performance of the molars of South Ronaldsay mice for crushing food items, despite the fact that the additional cusplet on the Papa Westray first upper molar can participate to the comminution of food particles. Functionally relevant dental differences between these populations could thus have arisen in a relatively short evolutionary time-span (maximum ~ 1200 years since the Viking colonization of Orkney).

How are Dental Differences Accommodated by the Jaw?

The next question was to know whether these differences in dental morphology were accompanied by differences in the rest of the masticatory apparatus. The mandible being the moving tool bringing teeth into occlusion, we quantified mandible shape and its mechanical advantages. Bite force
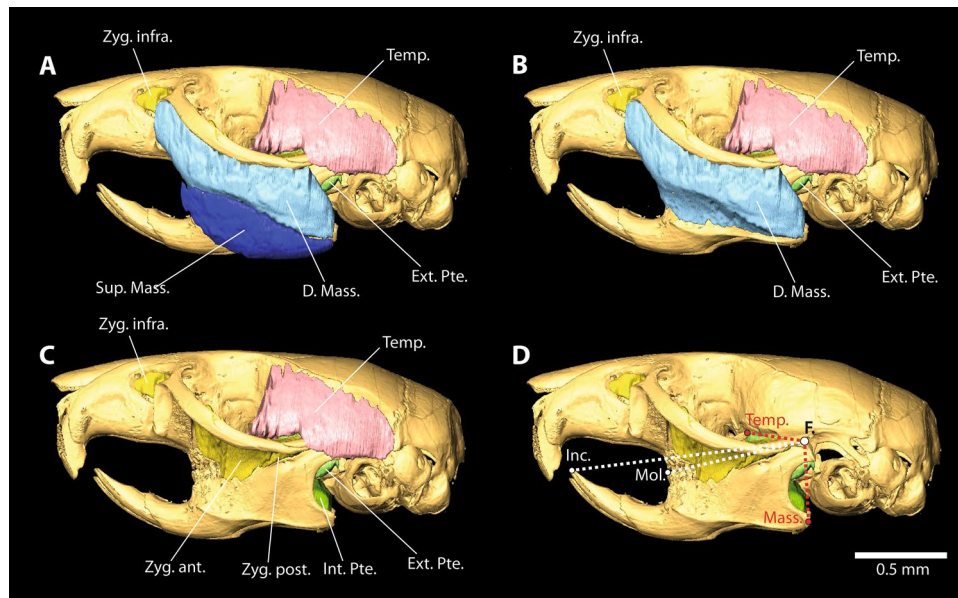
Fig. 8 Masticatory muscles and mechanical advantages of the mandibles. **a**–**c** Masticatory muscles, represented on a CT-scan visualization of a mouse skull (SR413): masseter in blue, temporal in pink, zygomaticomandibularis in yellow, and pterygoid in green. Some muscles (e.g. temporal and deep masseter) are composed of several parts that were discernable on dissection but not on segmentation of micro-CT images. These parts have been pooled for dissection and quantification. **d** Mechanical advantages, with in-levers (distance from the fulcrum to the point of muscle attachment; red dotted lines) and out-levers (distance from the fulcrum to the bite point; white dotted lines). *D. Mass.* deep masseter, *Ext. Pte.* external pterygoid; *F* fulcrum; *Inc* incisor; *Int. Pte.* internal pterygoid, *Mass.* masseter; *Mol* molar; *Sup. Mass.* superficial masseter; *Temp.* temporalis; *Zyg. ant.* anterior part of the zygomaticomandibularis; *Zyg. infra.* infraorbital part of the zygomaticomandibularis; *Zyg. post.* posterior part of the zygomaticomandibularis
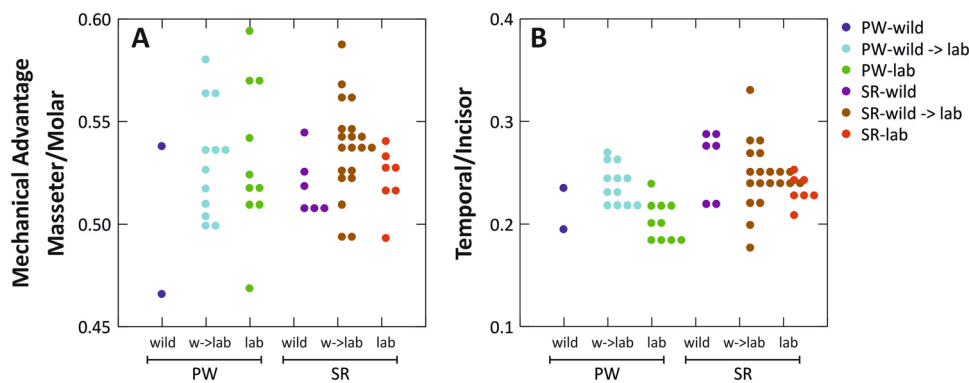
Fig. 9 Mechanical advantage of in-/out-lever ratios in wild-trapped PW and SR mice and their descendants in the lab. **a** Mechanical advantage of the temporal/incisor complex. **b** Mechanical advantage of the masseter/molar complex. Groups correspond, for the PW and SR strains, to wild animals trapped and sacrificed on the field (wild), wild animals brought back to the lab (wild → lab), and lab descendants (lab)

and the force of the main masticatory muscles were further assessed. No differences could be demonstrated between PW and SR mice, except for tenuous differences in mandible shape and the performance of the temporal/incisor complex, with lab PW displaying a lower temporal/incisor mechanical advantage. Wild PW also tended to display a lower temporal/incisor mechanical advantage than wild SR. However, a

lower mechanical advantage for the temporal/incisor complex may be unfavorable to force output but more favorable to speed at biting, as it is often the case in insectivorous taxa (Fabre et al. 2017).

The limited number of PW and SR lab specimens considered here may have been insufficient to evidence subtle fine-tuning of the masticatory apparatus to the important
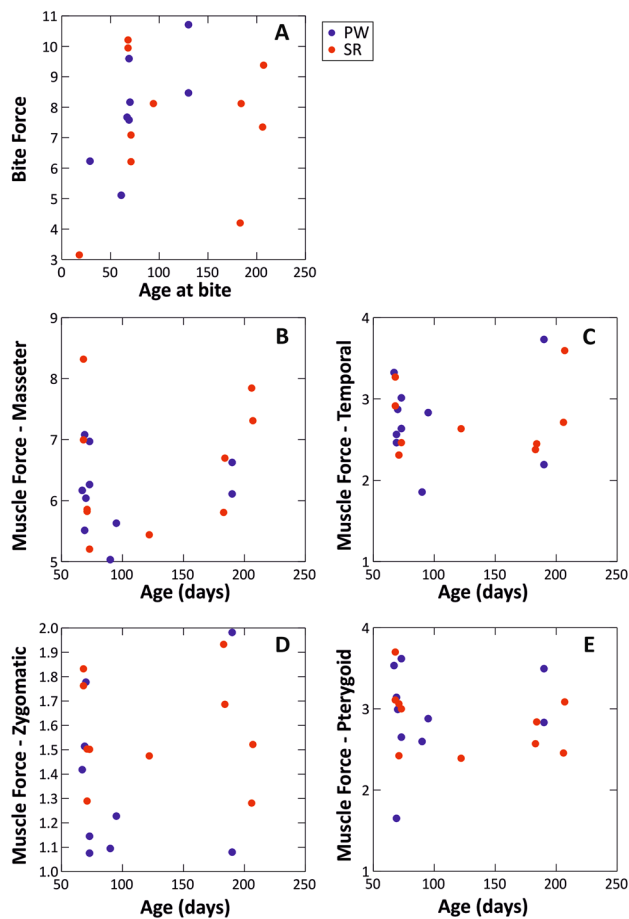
Fig. 10 Bite force, and force of the main masticatory muscles as a function of age in PW and SR lab mice. **a** Bite force in newtons. **b–e** Force of the main masticatory muscles, estimated from dissections

dental changes, but the results anyway show that differences in molar morphology do not always have to be accommodated by differences of the same magnitude in the jaw and masticatory muscles. Indeed, a hammer can perform various functions due to differences in its head shape, without differences in the handle. Evidences of mosaic evolution between molar and mandible shape have been provided by wood mice populations from various islands (Renaud and Michaux 2007), confirming the potential for uncoupling the evolution of both features, despite the need for integration of the jaw bone and the teeth (Zelditch et al. 2008) and evidence of constraints exerted by the jaw on the developing teeth (Renvoisé et al. 2017). This uncoupling may be favored by the fact that the dental changes occurring in PW did not affect the main pattern of propalinal occlusion, since the additional cusplet on PW first upper molars is located anterior to the occlusion with the lower molar. The rise of this morphological unusual phenotype in the Papa Westray and other Orkney populations (Ledevin et al. 2016) may thus exemplify a dental diversification in a constrained functional

context, allowing for an increase of the surface of contact with food items without requiring any further change of the masticatory system.

Mandible divergence might have been reduced in our study by the fact that all mice investigated were bred in the same laboratory environment and were fed with the same food. The mandible is constantly remodeled in response to muscular action and external forces, leading to significant differences between mice fed food of different consistency (Anderson et al. 2014; Renaud et al. 2010). Mice from PW and SR that have been bred at least for a part of their life under laboratory conditions, thus consuming the same food, displayed more similar mandible shapes than mice sacrificed at capture. Laboratory descendants seemed further shifted in a similar morphological direction, showing that disruptive selection for tooth morphology (with or without additional cusplet) had no disruptive effect on mandible morphology. Plasticity in response to common breeding conditions may also have contributed to the similar bite force and muscle force observed in the two strains. Possibly, PW mice were more sensitive to the environmental change represented by being in lab conditions, and/or to the selection acting upon the strain. This is suggested by the decrease in temporal/incisor mechanical advantage observed in the laboratory descendants of this strain, compared to both their wild ancestors and SR mice. This effect may have a behavioral component, underlining that behavior is part of a complex interplay involving also muscles, teeth and bones and leading to a co-adapted feeding apparatus (Anderson et al. 2014).

At this intraspecific level, plastic effects related to remodeling, including the response to food but also behavior and ageing, may be of the same magnitude as interpopulation differentiation, making it difficult to demonstrate consistent patterns. Breeding wild-derived strains should help to further separate heritable differences from plastic effects on jaw shape (Boell and Tautz 2011).

Conclusion

The two wild-derived strains from Papa Westray and South Ronaldsay exhibit important differences in tooth geometry. These differences may be functionally relevant, since they are associated with differences in dental complexity and sharpness, and traces of wear. To our knowledge, this is the first time that differences in functionally relevant topographic parameters are evidenced between populations of the same species. With its additional cusplet and reduction of the second and third molars, Papa Westray molar shape is reminiscent of phenotypes occurring, for instance, in some *Nannomys* pygmy mice such as *Mus minutoides* (Kan

Kouassi et al. 2008), which includes a substantial part of invertebrates in its diet (Happold 2013). The decrease of dental complexity observed in PW mice matches the signal associated, at a higher taxonomic level, with carnivorous taxa (Evans et al. 2007). In contrast, SR tooth morphology, displaying high complexity and high sharpness, seems adapted to the consumption of various and challenging food items. Differences in mandible morphology are small and more difficult to interpret, because they may be due to behavioral differences and plasticity in response to the lab environment.

The adaptive interpretation of these differences remains difficult because the two populations inhabit apparently similar commensal habitats. On both Papa Westray and South Ronaldsay, mice were trapped in commensal contexts, mostly agricultural buildings. Agricultural practices may differ, however, with traditional cattle breeding being the most important activity on Papa Westray whereas South Ronaldsay sustains more diverse exploitations including crop cultures. This may expose mice to more abundant resources of grain on South Ronaldsay. Not mutually exclusive, the two populations may differ in their degree of commensalism, and/or how they exploit human resources. Slight niche shifts may for instance have occurred on Papa Westray due to the coexistence of the mice with a potential competitor, the wood mouse (*Apodemus sylvaticus*) (Ledevin et al. 2016), but such interpretations remain hypothetical. Dental phenotypic changes as those evidenced on Papa Westray occur in different insular contexts (Ledevin et al. 2016; Renaud et al. 2011). Even if they may be occasionally mobilized by the screening of selection, they may have appeared in the populations due to random factors. Drift is likely increased in relatively small and isolated populations, and all the more on a small and remote island such as Papa Westray.

The evolution of Papa Westray mice may therefore illustrate the rise of an unusual phenotype, possibly occurring due to increased drift on a small and remote island. Inbreeding can cause rapid and pronounced morphological differentiation and even alter patterns of variance, covariance and integration (Jamniczky and Hallgrímsson 2011; Renaud et al. 2017) due to complex epistatic interactions and silencing of (co)variance-generating processes. The fact that the anterior elongation of the first upper molar, observed on Papa Westray specimens, was repeatedly evidenced in different contexts (insular evolution (Renaud et al. 2011) but also hybridization (Renaud et al. 2017)) suggest that the occurrence of such phenotypes could be favored by developmental lines of least resistance (Renaud et al. 2011).

Since the dental changes have a potential functional significance, the unusual phenotypes may enter the screening of selection, and participate to adaptation to local food resources. The evolution of these dental phenotypes was probably facilitated by the fact that they do not interfere with the complex requirements of the propalinal chewing movements and occlusion; hence, this dental evolution does not require an adjustment of the whole masticatory apparatus, including bones and muscles. The PW and SR populations exemplify once more that islands are 'laboratories of evolution' (Berry 1996). The two corresponding strains may help to get further insights into the evolutionary processes and mechanisms involved in this evolution.

Compliance with Ethical Standards

Conflict of interest The authors declare that they have no conflict of interest.

References

Abramoff, M. D., Magalhaes, P. J., & Ram, S. J. (2004). Image processing with imageJ. *Biophotonics International*, *11*(7), 36–42.

Anderson, P. S. L., Renaud, S., & Rayfield, E. J. (2014). Adaptive plasticity in the mouse mandible. *BMC Evolutionary Biology, 14*, 85.

Berry, R. J. (1996). Small mammal differentiation on islands. *Philosophical Transactions of the Royal Society, London B, 351*(1341), 753–764.

Boell, L., & Tautz, D. (2011). Micro-evolutionary divergence pattersn of mandible shapes in wild house mouse (*Mus musculus*) populations. *BMC Evolutionary Biology, 11*(306).

Bonhomme, V., Picq, S., Gaucherel, C., & Claude, J. (2014). Momocs: Outline analysis using R. *Journal of Statistical Software, 56*, 1–24.

Boyer, D. M. (2008). Relief index of second mandibular molars is a correlate of diet among prosimian primates and other euarchontan mammals. *Journal of Human Evolution, 55*, 1118–1137.

Boyer, D. M., Evans, A. R., & Jernvall, J. (2010). Evidence of dietary differentiation among late Paleocene–early Eocene plesiadapids (Mammalia, primates). *American Journal of Physical Anthropology, 142*, 194–210. https://doi.org/10.1002/ajpa.21211.

Boyer, D. M., Puente, J., Gladman, J. T., Glynn, C., Mukherjee, S., Yapuncich, G. S., et al. (2015). A new fully automated approach for aligning and comparing shapes. *The Anatomical Record, 298*(1), 249–276. http://www2.stat.duke.edu/~sayan/auto3dgm/.

Bunn, J. M., Boyer, D. M., Lipman, Y., Clair, E. M. S., Jernvall, J., & Daubechies, I. (2011). Comparing Dirichlet normal surface energy of tooth crowns, a new technique of molar shape quantification for dietary inference, with previous methods in isolation and in combination. *American Journal of Physical Anthropology, 145*, 247–261. https://doi.org/10.1002/ajpa.21489.

Champely, S. (2018). pwr: Basic functions for power analysis. R package version 1.2-2.

Charles, C., & Viriot, L. (2015). Variations and anomalies in rodent teeth and their importance for testing developmental models. In P. G. Cox & L. Hautier (Eds.), *Evolution of the rodents: Advances in phylogeny, functional morphology and development* (pp. 405–423). Cambridge: Cambridge University Press.

Crampton, J. S. (1995). Elliptic Fourier shape analysis of fossil bivalves: Some practical considerations. *Lethaia, 28*, 179–186.

de Winter, J. C. F. (2013). Using the student's *t*-test with extremely small sample sizes. *Practical Assessment, Research and Evaluation, 18*(10), 1–12.

Dray, S., & Dufour, A.-B. (2007). The ade4 package: Implementing the duality diagram for ecologists. *Journal of Statistical Software, 22*, 1–20.

Evans, A. R., & Jernvall, J. (2009). Patterns and constraints in carnivoran and rodent dental complexity and tooth size. In SVP program and abstracts book. *Journal of Vertebrate Paleontology, 29*, 92A.

Evans, A. R., & Sanson, G. D. (2003). The tooth of perfection: Functional and spatial constraints on mammalian tooth shape. *Biological Journal of the Linnean Society, 78*, 173–191.

Evans, A. R., Wilson, G. P., Fortelius, M., & Jernvall, J. (2007). High-level similarity of dentitions in carnivorans and rodents. *Nature, 445*(nature05433), 78–81. https://doi.org/10.1038/nature05433.

Fabre, P.-H., Herrel, A., Fitriana, Y., Meslin, L., & Hautier, L. (2017). Masticatory muscle architecture in a water-rat from Australasia (Murinae, *Hydromys*) and its implication for the evolution of carnivory in rodents. *Journal of Anatomy, 231*(3), 380–397.

Godfrey, L. R., Winchester, J. M., King, S. J., Boyer, D. M., & Jernvall, J. (2012). Dental topography indicates ecological contraction of lemur communities. *American Journal of Physical Anthropology, 148*, 215–227. https://doi.org/10.1002/ajpa.21615.

Gomes Rodrigues, H., Merceron, G., & Viriot, L. (2009). Dental microwear patterns of extant and extinct Muridae (Rodentia, Mammalia): Ecological implications. *Naturwissenschaften, 96*, 537–542.

Gunz, P., Mitteroecker, P., & Bookstein, F. L. (2005). Semilandmarks in three dimensions. Modern morphometrics in physical anthropology. In D. E. Slice (Ed.), *Modern morphometrics in physical anthropology: Developments in primatology: Progress and prospects* (pp. 73–98). New York: Springer.

Hammer, Ø, Harper, D. A. T., & Ryan, P. D. (2001). PAST: Paleontological Statistics software package for education and data analysis. *Palaeontological Electronica, 4*(1), 1–9.

Happold, D. C. D. (2013). *Mammals of Africa. Volume III: Rodents, hares and rabbits*. London: Bloomsbury Publishing.

Harmon, L. J., Kolbe, J. J., Cheverud, J. M., & Losos, J. B. (2005). Convergence and the multidimensional niche. *Evolution, 59*(2), 409–421.

Herrel, A., De Smet, A., Aguirre, L. F., & Aerts, P. (2008). Morphological and mechanical determinants of bite force in bats: Do muscles matter? *Journal of Experimental Biology, 211*, 86–91. https://doi.org/10.1242/jeb.012211.

Herrel, A., Spithoven, L., Van Damme, R., & De Vree, F. (1999). Sexual dimorphism of head size in *Gallotia galloti*: Testing the niche divergence hypothesis by functional analyses. *Functional Ecology, 13*(3), 289–297.

Hiiemae, K. M. (1971). The structure and function of the jaw muscles in the rat (*Rattus norvegicus* L.) III. The mechanics of the muscles. *Zoological Journal of the Linnean Society, 50*, 111–132.

Jacobs, L. L., Flynn, L. J., Downs, W. R., & Barry, J. C. (1990). *Quo vadis, Antemus?* The Siwalik Muroid record. In E. H. Lindsay (Ed.), *European neogene mammal chronology* (pp. 573–586). New York: Plenum Press.

Jamniczky, H. A., & Hallgrímsson, B. (2011). Modularity in the skull and cranial vasculature of laboratory mice: Implications for the evolution of complex phenotypes. *Evolution and Development, 13*(1), 28–37.

Jernvall, J. (2000). Linking develoment with generation of novelty in mammalian teeth. *Proceedings of the National Academy of Sciences, USA, 97*(6), 2641–2645.

Kan Kouassi, S., Nicolas, V., Aniskine, V., Lalis, A., Cruaud, C., Couloux, A., et al. (2008). Taxonomy and biogeography of the African Pygmy mice, Subgenus *Nannomys* (Rodentia, Murinae, *Mus*) in Ivory Coast and Guinea (West Africa). *Mammalia, 72*, 237–252.

Kavanagh, K. D., Evans, A. R., & Jernvall, J. (2007). Predicting evolutionary patterns of mammalian teeth from development. *Nature, 449*, 427–432.

Kuhl, F. P., & Giardina, C. R. (1982). Elliptic Fourier features of a closed contour. *Computer Graphics and Image Processing, 18*, 259–278.

Langsrud, Ø, & Mevik, B.-H. (2012). ffmanova: Fifty-fifty MANOVA. https://CRAN.R-project.org/package=ffmanova.

Lazzari, V., Charles, C., Tafforeau, P., Vianey-Liaud, M., Aguilar, J.-P., Jaeger, J.-J., et al. (2008). Mosaic convergence of rodent dentitions. *PLoS ONE, 3*, e3607.

Ledevin, R., Chevret, P., Ganem, G., Britton-Davidian, J., Hardouin, E. A., Chapuis, J.-L., et al. (2016). Phylogeny and adaptation shape the teeth of insular mice. *Proceedings of the Royal Society of London, Biological Sciences* (*series B*), *283*, 20152820, https://doi.org/10.1098/rspb.2015.2820.

Miller, G. S. (1912). *Catalogue of the mammals of Western Europe (exclusive of Russia) in the collection of the British Museum*. London: British Museum (Natural History).

Murphy, R. A., & Beardsley, A. C. (1974). Mechanical properties of the cat soleus muscle in situ. *American Journal of Physiology, 227*(5), 1008–1013.

Pampush, J. D., Winchester, J. M., Morse, P. E., Vining, A. Q., Boyer, D. M., & Kay, R. F. (2016). Introducing molaR: A new r package for quantitative topographic analysis of teeth (and other topographic surfaces). *Journal of Mammalian Evolution, 161*(4), 705–721. https://doi.org/10.1007/s10914-016-9326-0.

R-Core-Team (2017). *R: A language for environment and statistical computing*. Vienna, Austria: R Foundation for Statistical Computing.

Renaud, S., Alibert, P., & Auffray, J.-C. (2017). Impact of hybridization on shape, variation and covariation of the mouse molar. *Evolutionary Biology, 44*(1), 69–81.

Renaud, S., & Auffray, J.-C. (2013). The direction of main phenotypic variance as a channel to morphological evolution: Case studies in murine rodents. *Hystrix, The Italian Journal of Mammalogy, 24*(1), 85–93. https://doi.org/10.4404/hystrix-24.1-6296.

Renaud, S., Auffray, J.-C., & de La Porte, S. (2010). Epigenetic effects on the mouse mandible: Common features and discrepancies in remodeling due to muscular dystrophy and response to food consistency. *BMC Evolutionary Biology, 10*, 28. http://www.biomedcentral.com/1471-2148/10/28.

Renaud, S., & Ledevin, R. (2017). Impact of wear and diet on molar row geometry and topography in the house mouse. *Archives of Oral Biology, 81*, 31–40.

Renaud, S., Michaux, J., Jaeger, J.-J., & Auffray, J.-C. (1996). Fourier analysis applied to *Stephanomys* (Rodentia, Muridae) molars: Nonprogressive evolutionary pattern in a gradual lineage. *Paleobiology, 22*(2), 255–265.

Renaud, S., & Michaux, J. R. (2007). Mandibles and molars of the wood mouse, *Apodemus sylvaticus* (L.): Integrated latitudinal signal and mosaic insular evolution. *Journal of Biogeography, 34*(2), 339–355.

Renaud, S., Pantalacci, S., & Auffray, J.-C. (2011). Differential evolvability along lines of least resistance of upper and lower

molars in island house mice. *PLoS One, 6*(5), e18951. https://doi.org/10.1371/journal.pone.0018951.

Renaud, S., Pantalacci, S., Quéré, J.-P., Laudet, V., & Auffray, J.-C. (2009). Developmental constraints revealed by co-variation within and among molar rows in two murine rodents. *Evolution and Development, 11*(5), 590–602. https://doi.org/10.1111/j.1525-142X.2009.00365.x.

Renaud, S., Rodrigues, G., Ledevin, H., Pisanu, R., Chapuis, B., J.-L., & Hardouin, E. A. (2015). Fast morphological response of house mice to anthropogenic disturbances on a Sub-Antarctic island. *Biological Journal of the Linnean Society, 114*, 513–526.

Renvoisé, E., Kavanagh, K. D., Lazzari, V., Häkkinen, T. J., Rice, R., Pantalacci, S., et al. (2017). Mechanical constraint from growing jaw facilitates mammalian dental diversity. *Proceedings of the National Academy of Sciences, USA, 114*(35), 9403–9408.

Rohlf, F. J., & Archie, J. W. (1984). A comparison of Fourier methods for the description of wing shape in Mosquitoes (Diptera: Culicidae). *Systematic Zoology, 33*(3), 302–317.

Salazar-Ciudad, I., & Jernvall, J. (2002). A gene network model accounting for develoment and evolution of mammalian teeth. *Proceedings of the National Academy of Sciences, USA, 99*(12), 8116–8120.

Santana, S. E., Strait, S., & Dumont, E. R. (2011). The better to eat you with: Functional correlates of tooth structure in bats. *Functional Ecology, 25*, 839–847.

Schlager, S. (2016). mesheR: Meshing operations on triangular meshes. (0.4.160301 ed., pp. R package).

Schlager, S. (2017). Morpho and Rvcg: Shape analysis in {R}. In G. Zheng, S. Li, & G. Szekely (Eds.), Statistical shape and deformation analysis (pp. 217–256). Cambridge: Academic Press.

Schluter, D. (1996). Adaptive radiation along genetic lines of least resistance. *Evolution, 50*(5), 1766–1774.

Scoville, A. G., & Pfrender, M. E. (2010). Phenotypic plasticity facilitates recurrent rapid adaptation to introduced predators.

Proceedings of the National Academy of Sciences, USA, 107(9), 4260–4263.

Searle, J. B., Jones, C. S., Gündüz, İ, Scascitelli, M., Jones, E. P., Herman, J. S., et al. (2009). Of mice and (Viking?) men: Phylogeography of British and Irish house mice. *Proceedings of the Royal Society of London, Biological Sciences* (*series B*), *276*, 201–207. https://doi.org/10.1098/rspb.2008.0958.

Sheets, H. D., Covino, K. M., Panasiewicz, J. M., & Morris, S. R. (2006). Comparison of geometric morphometric outline methods in the discrimination of age-related differences in feather shape. *Frontiers in Zoology, 3*, 15. https://doi.org/10.1186/1742-9994-3-15.

Skinner, M. M., & Gunz, P. (2010). The presence of accessory cusps in chimpanzee lower molars is consistent with a patterning cascade model of development. *Journal of Anatomy, 217*, 245–253.

Stoetzel, E., Denys, C., Michaux, J., & Renaud, S. (2013). *Mus* in Morocco: A quaternary sequence of intraspecific evolution. *Biological Journal of the Linnean Society, 109*, 599–621.

Ungar, P. S. (2004). Dental topography and diets of *Australopithecus afarensis* and early *Homo. Journal of Human Evolution, 46*, 605–622. https://doi.org/10.1016/j.jhevol.2004.03.004.

West-Eberard, M. J. (1989). Phenotypic plasticity and the origin of diversity. *Annual Review of Ecology, Evolution and Systematics, 20*, 249–278.

Winchester, J. M., Boyer, D. M., Clair, E. M. S., Gosselin-Ildari, A. D., Cooke, S. B., & Ledogar, J. A. (2014). Dental topography of platyrrhines and prosimians: Convergence and contrasts. *American Journal of Physical Anthropology, 153*(1), 29–44. https://doi.org/10.1002/ajpa.22398.

Wood, A. E. (1965). Grades and clades among rodents. *Evolution, 19*, 115–130.

Zelditch, M. L., Wood, A. R., Bonett, R. M., & Swiderski, D. L. (2008). Modularity of the rodent mandible: Integrating bones, muscles, and teeth. *Evolution and Development, 10*(6), 756–766.